Photonic crystal microcavities for cavity quantum electrodynamics with a single quantum dot

Jelena Vučković[a] and Yoshihisa Yamamoto
Quantum Entanglement Project, ICORP, JST, Ginzton Laboratory, Stanford University, Stanford, California 94305

(Received 10 October 2002; accepted 19 February 2003)

We propose a planar photonic crystal microcavity design specially tailored for cavity quantum electrodynamics with a single quantum dot emitter embedded in semiconductor. With quality factor up to 45 000, mode volume smaller than a cubic optical wavelength in material, and electric field maximum located in the high-refractive index region at the cavity center, this design can enable both strong coupling and lasing with a single quantum dot exciton. The achievable range of the quality factor to mode volume ratios and the feasible fabrication of the proposed structure make it favorable to other semiconductor microcavities. © *2003 American Institute of Physics.*
[DOI: 10.1063/1.1567824]

The observation of cavity quantum electrodynamics (CQED) phenomena in semiconductor systems, such as a single quantum dot (QD) strongly coupled to electromagnetic field or single-dot lasing, relies on the construction of optical microcavities with high quality factors (Q) and small mode volumes (V). Most of the semiconductor CQED research to date has been focused on distributed-Bragg-reflector (DBR) microposts[1,2] or microdisk microcavities,[3,4] with a recent exception of preliminary photonic crystal microcavity work.[5] Due to the limitations of employed fabrication methods, or the lack of right designs, the aforementioned phenomena have not been exhibited so far. Even for those quantum optical devices that have been demonstrated (e.g., single-photon sources based on pulsed excitation of a QD)[6–8] any microcavity improvement can lead to a desirable increase in the device efficiency and speed. We have recently proposed the optimized designs of DBR microposts potentially enabling the observation of the single QD CQED phenomena.[9] However, stringent fabrication requirements of these structures motivated us to investigate planar photonic crystal microcavities as a more robust and manufacturable solution.

The design and fabrication of photonic crystal microcavities that can enable strong coupling regime with a neutral atom trapped in one of photonic crystal holes have been proposed recently.[10,11] These extremely high Q/V structures can have Q factors larger than 10^4 together with mode volumes of the order of one-half of the cubic optical wavelength in material $[1/2(\lambda/n)^3]$. Q factor close to 3000 has been subsequently demonstrated from such a cavity where theory predicts $Q \approx 4000$,[12] and the lowest-threshold lasing at 1.5 μm has been observed from optically pumped multi-quantum wells embedded in it.[13] Moreover, by employing inversion methods, the theoretical Q factor of this design has been increased even further, to a value around 10^5.[14] However, as these structures have been optimized for interaction with neutral atoms, they have electric field maximum in the air region and are therefore not suitable for interaction with a single QD emitter embedded in semiconductor. Other high-Q photonic crystal cavity designs that have recently appeared in the literature are also not tailored for semiconductor CQED, since they have a node of electric field in the high-index region at the cavity center or an increased mode volume.[15–17] In this letter, we present a design that could enable very high Q/V ratios, but with electric field maximum in the high-index region at the cavity center, to facilitate its alignment to a QD and prevent nonradiative surface recombination. Although we have been primarily motivated by a single QD CQED experiment, this design can also be employed to significantly reduce the lasing threshold of standard photonic crystal lasers.

The proposed microcavity is illustrated in Fig. 1. The structure is formed in the underlying planar hexagonal photonic crystal with lattice periodicity a and hole radius r, constructed in the slab with refractive index n and thickness d in the z direction. As illustrated in the figure on the left, the central hole is omitted and its two nearest neighbors along the x axis are made ellipsoidal with major axis equal to A and minor axis equal to $2r$. The edge-to-edge distance be-

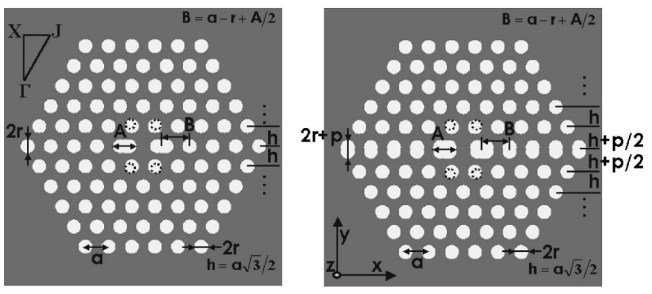

FIG. 1. Photonic crystal microcavity for cavity quantum electrodynamics with a single quantum dot emitter embedded in semiconductor. After omitting the central hole and modifying its nearest-neighbors (as shown in the figure on the left), fractional edge dislocations are inserted along the x axis to tune the Q factor of the x-dipole mode (figure on the right). The orientation of x, y, and z axes is indicated in the plot, and the point (0,0,0) is located laterally at the center of the defect and vertically in the middle of the slab.

[a]Also at: Department of Electrical Engineering, Stanford University, Stanford, CA 94305; electronic mail: jela@stanford.edu

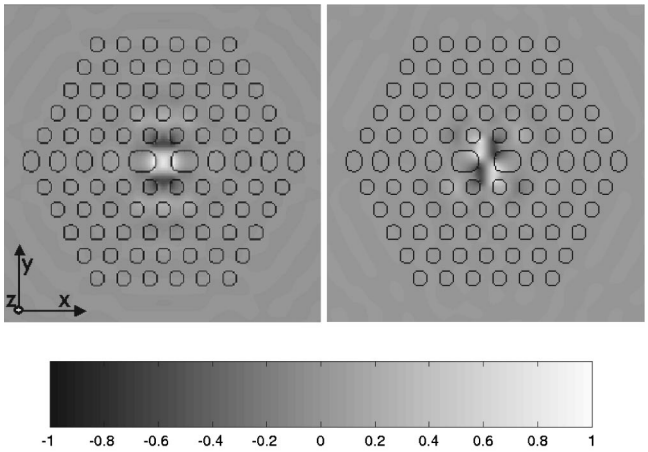

FIG. 2. Electric field components of the x-dipole mode in the middle of the slab for the microcavity from Fig. 1. The figure on the left corresponds to the x component, and the figure on the right to the y component of electric field (the z component is equal to zero at this plane). Electric field is maximum and is x polarized at the cavity center, where an emitter should be located in order to provide a strong interaction. The parameters of this particular cavity are $r/a=0.3$, $d/a=0.65$, $n=3.4$, $A/r=3.33$, and $p/a=0.2$, leading to the Q factor larger than 5000 together with the mode volume of $1/2(\lambda/n)^3$ with only seven photonic crystal layers around the defect.

tween the ellipses and their next-nearest neighbor holes along the x axis is preserved and is equal to $a-2r$. In order to tune the Q factor of the x-dipole mode (whose electric field pattern is shown in Fig. 2), fractional edge dislocations of the order p are then applied along the x axis, as illustrated on the right of Fig 1. Fractional edge dislocations and their effect on the Q-factor improvement of the x-dipole mode have been described in more detail in our earlier publications.[10,11] Briefly, by inserting them, one can perform small adjustments to the central lobe size of the even field components (E_x and B_y), without significantly perturbing mode volume and photonic crystal reflectivity. This in turn results in cancellation of the Fourier components within the light cone and consequent suppression of radiation losses when the balance between the positive and negative field lobes is reached.

Figure 3 displays Q factor and frequency a/λ of the x-dipole mode in the structure from Fig. 1, as a function of p/a and A. The underlying hexagonal photonic crystal parameters are $r/a=0.3$, $d/a=0.65$, and $n=3.4$, with a photonic band gap for the TE-like (even) modes extending roughly from $a/\lambda=0.26$ to 0.33. In order to minimize the computational requirements of the employed finite-difference time-domain method, we have analyzed structures with only five photonic crystal layers around the defect. Q factor can be expressed as $Q=Q_{\parallel}Q_{\perp}/(Q_{\parallel}+Q_{\perp})$, where $Q_{\perp}$ corresponds to the radiation losses above the surface of the membrane, for $|z|>3d/2$, and $Q_{\parallel}$ includes only the in-plane losses within the membrane, for $|z|<3d/2$. By increasing the number of photonic crystal layers above 5, the in-plane losses are suppressed, while the out-of-plane (radiation) losses remain approximately unchanged; $Q_{\parallel}$ becomes consequently much larger than $Q_{\perp}$, leading to the Q factor being determined only by the radiation losses, $Q\approx Q_{\perp}$.[10,11] For structures operating away from the band gap edges, such as the peak-Q point in Fig. 3 with electric field pattern shown in Fig. 2, the condition of $Q\approx Q_{\perp}$ can be achieved with as few as seven photonic crystal layers. The Q factor can therefore be larger than 5000 at its peak, while the mode volume remains roughly equal to one half of the cubic optical wavelength $[1/2(\lambda/n)^3]$ in the studied range of p. The significance of the two ellipsoidal holes next to the defect region is clear from Fig. 3: without them (i.e., for $A/r=2$), the resonant mode frequency is too low, and it exits the band gap before the out-of-plane losses are minimized by tuning p. As we have noted previously,[10] the resonant mode frequency drops as a function of the elongation parameter p; it is therefore important to start in the elongation process as close to the top of the photonic band gap as possible, in order to minimize the out-of-plane losses within the band gap and thus preserve a strong in-plane confinement and a small mode volume. By making the two central holes ellipsoidal and increasing A, the resonant mode's overlap with air region increases, thereby increasing its frequency and leaving enough space for the Q optimization within the band gap (see Fig. 3).

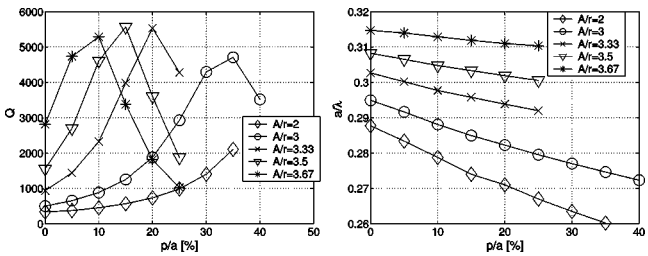

FIG. 3. $Q_{\perp}$ factor (left) and normalized frequency a/λ (right) of the x-dipole mode as a function of the normalized elongation parameter p/a, for the cavity design from Fig. 1. The underlying hexagonal photonic crystal parameters are $r/a=0.3$, $d/a=0.65$, and $n=3.4$, leading to the band gap for even modes extending from $a/\lambda=0.26$ to 0.33. Various plots correspond to different values of the major axis A of the two ellipsoidal holes next to the defect region in the x direction. For the peak-Q point, $Q\approx Q_{\perp}$ can be achieved with as few as seven photonic crystal layers around the defect.

Further improvement in the Q factor can be achieved by tuning the four holes closest to the defect in the ΓJ directions, as illustrated with dotted lines in Fig. 1. The radius of the four holes is reduced to r_1, and they are simultaneously shifted by $r-r_1$ in the ΓJ directions to preserve their edge-to-edge distance from the next-nearest neighbor holes and thus keep a high photonic crystal reflectivity in these directions. The tuning of these four holes as a tool for increasing the Q factor of the dipole mode has been explored earlier.[10,14] In this case, the mechanism behind the Q improvement is the suppression of radiation losses due to mode delocalization.[17] As expected, the mode volume of the resonant x-dipole mode increases slightly to $0.8(\lambda/n)^3$, but the Q factor is improved to 45 000, the best Q/V ratio by a factor of 6. This maximum is obtained in the structure with $A/r=3.33$, $p/a=0$, $r_1/a=0.25$, $r/a=0.3$, $d/a=0.65$, $n=3.4$, and $a/\lambda=0.2847$.

Let us consider the cavity with the peak Q/V ratio and assume that it operates at $\lambda\approx 900$ nm, on resonance with an InAs/GaAs QD exciton whose radiative lifetime without a cavity is equal to 0.5 ns. If the exciton is initially slightly detuned from the cavity resonance, it can be easily brought to it by varying the sample temperature.[18] The cavity field decay rate is $\kappa=(\pi c)/(\lambda Q)=23$ GHz, and the spontaneous emission rate of the exciton without a cavity is $\Gamma=2$ GHz.

The homogenous linewidth (γ_h) of excitons on our samples is typically of the order of a few gigahertz (e.g., 2 GHz), and therefore smaller than the cavity field decay rate κ. The Rabi frequency g_0 can be expressed as $g_0=\Gamma/2n\sqrt{V_0/V}$ where $V_0=(3c\lambda^2)/(2\pi\Gamma n)$.[9] Hence, the photonic crystal cavity-QD exciton system on resonance has g_0 equal to 315 GHz. For an exciton located at the electric field maximum and aligned with the field, a very strong coupling (high-Q regime) is possible, as the coupling parameter g is much larger than the decay rates of the system: $g=g_0\gg\kappa,\pi\gamma_h$. Moreover, strong coupling is possible even if the ratio of g to κ is reduced by another factor of 14, due to the misalignment between the QD and the field maximum or the reduction in the Q factor resulting from fabrication inaccuracies or material absorption. As an example, even if the QD is positioned at one-half of the electric field maximum, and the Q factor is up to seven times smaller than the theoretically predicted value of 45 000, the strong coupling would occur. Despite this robustness of the proposed design, we are also developing a fabrication method that would enable to lithographically align a microcavity to the location of a QD previously selected during the spectroscopy performed on unprocessed wafers. With such alignment, the minimum Q factor necessary to achieve the strong coupling would be approximately equal to 3000, which is in the range of already demonstrated experimental values for similar photonic crystal cavities.[12]

A single-QD laser represents an ultimate microscopic limit for semiconductor lasers; its realization would allow physical investigations similar to those afforded by the single-atom laser.[19] Lasing of such a system would occur when the exciton radiative lifetime is shorter than the cavity photon lifetime.[9] The cavity photon lifetime of the presented design with the Q factor of 45 000 is roughly 20 ps, which implies that a Purcell factor of 25 is necessary to initiate lasing with an exciton whose radiative lifetime without a cavity is 0.5 ns. Due to extremely small mode volume and large Q factor of this cavity, the needed Purcell factor should be easily achievable for an exciton located away from the field maximum, to prevent strong coupling.

In conclusion, we have proposed the design of a planar photonic crystal microcavity for CQED with a single QD emitter embedded in semiconductor. Although further optimization of this design is probably possible (e.g., by applying the inverse-problem approach of Ref. 14), the g/κ ratio for a typical QD exciton located at the center of this cavity is already 14 times above threshold of the high-Q regime. In other words, strong coupling is possible even when this ratio is reduced by more than an order of magnitude due to fabrication inaccuracies.

[1] J. M. Gérard, B. Sermage, B. Gayral, B. Legrand, E. Costard, and V. Thierry-Mieg, Phys. Rev. Lett. **81**, 1110 (1998).
[2] G. S. Solomon, M. Pelton, and Y. Yamamoto, Phys. Rev. Lett. **86**, 3903 (2001).
[3] B. Gayral, J. M. Gérard, A. Lematre, C. Dupuis, L. Manin, and J. L. Pelouard, Appl. Phys. Lett. **75**, 1908 (1999).
[4] A. Kiraz, P. Michler, C. Becher, B. Gayral, A. Imamoglu, L. Zhang, E. Hu, W. V. Schoenfeld, and P. M. Petroff, Appl. Phys. Lett. **78**, 3932 (2001).
[5] T. D. Happ, I. I. Tartakovskii, V. D. Kulakovskii, J. P. Reithmaier, M. Kamp, and A. Forchel, Phys. Rev. B **66**, 041303 (2002).
[6] C. Santori, M. Pelton, G. Solomon, Y. Dale, and Y. Yamamoto, Phys. Rev. Lett. **86**, 1502 (2001).
[7] P. Michler, A. Kiraz, C. Becher, W. V. Schoenfeld, P. M. Petroff, L. Zhang, E. Hu, and A. Imamoğlu, Science **290**, 2282 (2000).
[8] E. Moreau, I. Robert, J. M. Gérard, I. Abram, L. Manin, and V. Thierry-Mieg, Appl. Phys. Lett. **79**, 2865 (2001).
[9] J. Vučković, M. Pelton, A. Scherer, and Y. Yamamoto, Phys. Rev. A **66**, 023808 (2002).
[10] J. Vučković, M. Lončar, H. Mabuchi, and A. Scherer, Phys. Rev. E **65**, 016608 (2002).
[11] J. Vučković, M. Lončar, H. Mabuchi, and A. Scherer, IEEE J. Quantum Electron. **38**, 850 (2002).
[12] T. Yoshie, J. Vučković, A. Scherer, H. Chen, and D. Deppe, Appl. Phys. Lett. **79**, 4289 (2001).
[13] M. Lončar, T. Yoshie, A. Scherer, P. Gogna, and Y. Qui, Appl. Phys. Lett. **81**, 2680 (2002).
[14] J. M. Geremia, J. Williams, and H. Mabuchi, Phys. Rev. E **66**, 066606 (2002).
[15] H. Y. Ryu, H. G. Park, and Y. H. Lee, IEEE J. Sel. Top. Quantum Electron. **8**, 891 (2002).
[16] H. Y. Ryu, S. H. Kim, H. G. Park, J. K. Hwang, Y. H. Lee, and J. S. Kim, Appl. Phys. Lett. **80**, 3883 (2002).
[17] S. G. Johnson, S. Fan, A. Mekis, and J. D. Joannopoulos, Appl. Phys. Lett. **78**, 3388 (2001).
[18] J. Vučković, D. Fattal, C. Santori, G. Solomon, and Y. Yamamoto (unpublished).
[19] K. An, J. J. Childs, R. R. Dasari, and M. S. Feld, Phys. Rev. Lett. **73**, 3375 (1994).